

# The Study of the contribution of the LHT model to $Zb\bar{b}$ coupling

Bingfang Yang<sup>1,2</sup>, Xuelei Wang<sup>1</sup>, and Jinzhong Han<sup>1</sup>

<sup>1</sup> *College of Physics and Information Engineering,  
Henan Normal University, Xinxiang 453007, China*

<sup>2</sup> *Basic Teaching Department, Jiaozuo University, Jiaozuo 454000, China*

## Abstract

In the framework of the Littlest Higgs Model with T-parity (LHT), we study the contributions of the new particles to  $Zb\bar{b}$  couplings at one-loop level. Based on these results, we further study the branching ratio  $R_b$  and the unpolarized forward-backward asymmetry  $A_{FB}^b$ . We find that the correction of the new particles to  $Zb\bar{b}$  couplings is mainly on the left-handed coupling and has small part of the parameter space to alleviate the deviation between theoretical predictions and experimental values. The precision measurement value of  $R_b$  can give severe constraints on the relevant parameters. The constraints from the precision measurement value of  $A_{FB}^b$  are very weak.

PACS numbers: 14.65.Fy,12.60.-i,12.15.Mm,13.85.Lg

## I. INTRODUCTION

The Standard Model (SM) has been very successful, however, it is still believed to be a theory effective at the electroweak scale and some new physics (NP) must exist at higher energy regimes. So far there have been many speculations on the possible forms of the NP beyond the SM, one of the interesting possibilities is the Little Higgs model. The little Higgs theory was proposed [1] as a possible solution to the hierarchy problem and remains a popular candidate for the NP. The Littlest Higgs (LH) model [2] is a cute economical implementation of the little Higgs, but suffered from severe constraints from electroweak precision tests [3], which would require raising the mass scale of the new particles to far above TeV scale and thus reintroduce the fine-tuning in the Higgs potential [4]. The most serious constraints resulted from the tree-level corrections to precision electroweak observables due to the exchanges of the additional heavy gauge bosons present in the theories, as well as from the small but non-vanishing vacuum expectation value (VEV) of an additional weak-triplet scalar field. In order to solve this problem, a discrete symmetry called T-parity is proposed [5], which explicitly forbids any tree-level contributions from the heavy gauge bosons to the observables involving only the SM particles as external states. The interactions that induce triplet VEV contributions is also forbidden. This model is called the Littlest Higgs Model with T-parity (LHT). In the LHT model, corrections to the precision electroweak observables are generated exclusively at loop level.

The branching ratio  $R_b$  is very sensitive to the NP beyond the SM, the precision experimental value of  $R_b$  may give a severe constraint on the NP [6]. Experimentally, the electroweak observables have been precisely measured at the SLC and LEP, in the most recent analysis of the electroweak data,  $R_b = 0.21629 \pm 0.00066$  differs from the SM fit by  $0.7\sigma$ ,  $A_{FB}^b = 0.0992 \pm 0.0016$  disagrees with the SM fit by  $-2.9\sigma$  [7]. Furthermore, the experimental value of  $Zb\bar{b}$  couplings disagrees with the SM fit by about  $3\sigma$ , especially the deviation of the right-handed coupling is so large that it is very difficult to explain. These significant deviations from the  $A_{FB}^b$  and the  $Zb\bar{b}$  couplings might be the first window into the NP. With the running of the LHC, they will be further researched. In the LHT model, there are new fermions and new gauge bosons, which can contribute to the  $Zb\bar{b}$  couplings and give modifications to the  $R_b$  and  $A_{FB}^b$ . Therefore, it is possible to give some constraints on the relevant parameters via their radiative corrections to the  $R_b$  and  $A_{FB}^b$ .

In this paper, we calculate the contributions of the LHT model to the  $Zb\bar{b}$  couplings. On this basis, we further study the  $R_b$  and  $A_{FB}^b$ , then we give the constraints on the relevant parameters according to the precision measurements.

This paper is organized as follows. In Sec.II we recapitulate the LHT model and discuss the new flavor interactions which will contribute to the  $Zb\bar{b}$  vertex. In Sec.III we calculate the one-loop contributions of the LHT model to the  $Zb\bar{b}$  vertex,  $R_b$  and  $A_{FB}^b$ , then the relevant numerical results are shown. Finally, we give our conclusions in Sec.IV.

## II. A BRIEF REVIEW OF THE LHT MODEL

The LHT [5] is based on a non-linear sigma model describing the spontaneous breaking of a global  $SU(5)$  down to a global  $SO(5)$ . This symmetry breaking takes place at the scale  $f \sim \mathcal{O}(TeV)$  and originates from the VEV of an  $SU(5)$  symmetric tensor  $\Sigma$ , given by

$$\Sigma_0 \equiv \langle \Sigma \rangle = \begin{pmatrix} 0_{2 \times 2} & 0 & 1_{2 \times 2} \\ 0 & 1 & 0 \\ 1_{2 \times 2} & 0 & 0_{2 \times 2} \end{pmatrix} \quad (1)$$

From the  $SU(5)/SO(5)$  breaking, there arise 14 Goldstone bosons which are described by the ‘‘pion’’ matrix  $\Pi$ , given explicitly by

$$\Pi = \begin{pmatrix} -\frac{\omega^0}{2} - \frac{\eta}{\sqrt{20}} & -\frac{\omega^+}{\sqrt{2}} & -i\frac{\pi^+}{\sqrt{2}} & -i\phi^{++} & -i\frac{\phi^+}{\sqrt{2}} \\ -\frac{\omega^-}{\sqrt{2}} & \frac{\omega^0}{2} - \frac{\eta}{\sqrt{20}} & \frac{v+h+i\pi^0}{2} & -i\frac{\phi^+}{\sqrt{2}} & \frac{-i\phi^0+\phi^P}{\sqrt{2}} \\ i\frac{\pi^-}{\sqrt{2}} & \frac{v+h-i\pi^0}{2} & \sqrt{4/5}\eta & -i\frac{\pi^+}{\sqrt{2}} & \frac{v+h+i\pi^0}{2} \\ i\phi^{--} & i\frac{\phi^-}{\sqrt{2}} & i\frac{\pi^-}{\sqrt{2}} & -\frac{\omega^0}{2} - \frac{\eta}{\sqrt{20}} & -\frac{\omega^-}{\sqrt{2}} \\ i\frac{\phi^-}{\sqrt{2}} & \frac{i\phi^0+\phi^P}{\sqrt{2}} & \frac{v+h-i\pi^0}{2} & -\frac{\omega^+}{\sqrt{2}} & \frac{\omega^0}{2} - \frac{\eta}{\sqrt{20}} \end{pmatrix} \quad (2)$$

Under T-parity the SM Higgs doublet,  $H = (-i\pi^+\sqrt{2}, (v+h+i\pi^0)/2)^T$  is T-even while other fields are T-odd.

The Goldstone bosons  $\omega^\pm, \omega^0, \eta$  are respectively eaten by the new T-odd gauge bosons  $W_H^\pm, Z_H, A_H$ , which obtain masses at  $\mathcal{O}(v^2/f^2)$

$$M_{W_H} = M_{Z_H} = gf\left(1 - \frac{v^2}{8f^2}\right), M_{A_H} = \frac{g'f}{\sqrt{5}}\left(1 - \frac{5v^2}{8f^2}\right) \quad (3)$$

with  $g$  and  $g'$  being the SM  $SU(2)$  and  $U(1)$  gauge couplings, respectively.

The Goldstone bosons  $\pi^\pm, \pi^0$  are eaten by the T-even  $W_L^\pm$  and  $Z_L$  bosons of the SM, which obtain masses at  $\mathcal{O}(v^2/f^2)$

$$M_{W_L} = \frac{gv}{2}\left(1 - \frac{v^2}{12f^2}\right), M_{Z_L} = \frac{gv}{2\cos\theta_W}\left(1 - \frac{v^2}{12f^2}\right) \quad (4)$$

The photon  $A_L$  is also T-even and remains massless.

For each SM fermion, a copy of mirror fermion with T-odd quantum number is added in order to preserve the T-parity. For the mirror quarks, we denote them by  $u_H^i, d_H^i$ , where  $i=1, 2, 3$  are the generation index. At the order of  $\mathcal{O}(v^2/f^2)$  their masses are given by

$$m_{d_H^i} = \sqrt{2}\kappa_i f, m_{u_H^i} = m_{d_H^i}\left(1 - \frac{v^2}{8f^2}\right) \quad (5)$$

where  $\kappa_i$  are the diagonalized Yukawa couplings of the mirror quarks.

In order to cancel the quadratic divergence of the Higgs mass induced by top loops, an additional heavy quark  $T^+$  is introduced, which is even under T-parity. The implementation of T-parity then requires also a T-odd partner  $T^-$ . Their masses are given by

$$m_{T^+} = \frac{f}{v} \frac{m_t}{\sqrt{x_L(1-x_L)}} \left[1 + \frac{v^2}{f^2} \left(\frac{1}{3} - x_L(1-x_L)\right)\right] \quad (6)$$

$$m_{T^-} = \frac{f}{v} \frac{m_t}{\sqrt{x_L}} \left[1 + \frac{v^2}{f^2} \left(\frac{1}{3} - \frac{1}{2}x_L(1-x_L)\right)\right] \quad (7)$$

where  $x_L$  is the mixing parameter between the SM top-quark  $t$  and the new top-quark  $T^+$ .

Just like the SM, the mirror sector in the LHT model also has weak mixing, parameterised by unitary mixing matrices: two for mirror quarks and two for mirror leptons:

$$V_{Hu}, V_{Hd}, V_{Hl}, V_{H\nu} \quad (8)$$

$V_{Hu}$  and  $V_{Hd}$  are for the mirror quarks which are present in our analysis.  $V_{Hu}$  and  $V_{Hd}$  satisfy the physical constraints  $V_{Hu}^\dagger V_{Hd} = V_{CKM}$ . We follow [8] to parameterize  $V_{Hd}$  with three angles  $\theta_{12}^d, \theta_{23}^d, \theta_{13}^d$  and three phases  $\delta_{12}^d, \delta_{23}^d, \delta_{13}^d$

$$V_{Hd} = \begin{pmatrix} c_{12}^d c_{13}^d & s_{12}^d c_{13}^d e^{-i\delta_{12}^d} & s_{13}^d e^{-i\delta_{13}^d} \\ -s_{12}^d c_{23}^d e^{i\delta_{12}^d} - c_{12}^d s_{23}^d s_{13}^d e^{i(\delta_{13}^d - \delta_{23}^d)} & c_{12}^d c_{23}^d - s_{12}^d s_{23}^d s_{13}^d e^{i(\delta_{13}^d - \delta_{12}^d - \delta_{23}^d)} & s_{23}^d c_{13}^d e^{-i\delta_{23}^d} \\ s_{12}^d s_{23}^d e^{i(\delta_{12}^d + \delta_{23}^d)} - c_{12}^d c_{23}^d s_{13}^d e^{i\delta_{13}^d} & -c_{12}^d s_{23}^d e^{i\delta_{23}^d} - s_{12}^d c_{23}^d s_{13}^d e^{i(\delta_{13}^d - \delta_{12}^d)} & c_{23}^d c_{13}^d \end{pmatrix} \quad (9)$$

### III. THE ONE-LOOP CORRECTIONS TO $Zb\bar{b}$ COUPLINGS IN THE LHT MODEL

We employ the following notation for the effective  $Zb\bar{b}$  interaction:

$$\begin{aligned} L_{Zb\bar{b}} &= \frac{e}{S_W C_W} (g_L^b \bar{b} \gamma^\mu b P_L + g_R^b \bar{b} \gamma^\mu b P_R) Z_\mu \\ &= \frac{e}{2S_W C_W} \bar{b} \gamma^\mu (g_V^b - g_A^b \gamma_5) b Z_\mu \end{aligned} \quad (10)$$

where  $\theta_W$  is the Weinberg angle,  $S_W = \sin \theta_W$ ,  $C_W = \cos \theta_W$ ,  $P_L = \frac{1-\gamma_5}{2}$  and  $P_R = \frac{1+\gamma_5}{2}$ .

The effective couplings are then written as

$$\bar{g}_{L,R}^b = g_{L,R}^b + \delta g_{L,R}^{SM} + \delta g_{L,R}^{NP} \quad (11)$$

$$\bar{g}_{V,A}^b = g_{V,A}^b + \delta g_{V,A}^{SM} + \delta g_{V,A}^{NP} \quad (12)$$

where  $\bar{g}_{L,R}^b, \bar{g}_{V,A}^b$  are respectively the radiatively-corrected effective couplings,  $g_{L,R}^b$  are respectively the left-handed and right-handed  $Zb\bar{b}$  couplings at tree level,  $\delta g_{L,R}^{SM}$  and  $\delta g_{L,R}^{NP}$  are their corresponding one-loop corrections of the SM and the NP,  $g_{V,A}^b$  are respectively the vector and axial vector coupling coefficients of  $Zb\bar{b}$  interaction at tree level,  $\delta g_{V,A}^{SM}$  and  $\delta g_{V,A}^{NP}$  are their corresponding one-loop corrections of the SM and the NP. The tree-level couplings are given by

$$g_L^b = -\frac{1}{2} + \frac{1}{3} S_W^2 \quad , \quad g_R^b = \frac{1}{3} S_W^2 \quad (13)$$

$$g_V^b = g_L^b + g_R^b = -\frac{1}{2} + \frac{2}{3} S_W^2 \quad , \quad g_A^b = g_L^b - g_R^b = -\frac{1}{2} \quad (14)$$

The branching ratio is defined as

$$R_b = \frac{\Gamma(Z \rightarrow b\bar{b})}{\Gamma(Z \rightarrow \text{hadrons})} \quad (15)$$

The full hadron width is the sum of widths of five quark channels:

$$\Gamma(Z \rightarrow \text{hadrons}) = \Gamma(Z \rightarrow u\bar{u}) + \Gamma(Z \rightarrow d\bar{d}) + \Gamma(Z \rightarrow s\bar{s}) + \Gamma(Z \rightarrow c\bar{c}) + \Gamma(Z \rightarrow b\bar{b}) \quad (16)$$

For the decays to any of the five pairs of quarks  $q\bar{q}$  we have[9]

$$\Gamma_q \equiv \Gamma(Z \rightarrow q\bar{q}) = 12\Gamma_0 (g_{Aq}^2 R_{Aq} + g_{Vq}^2 R_{Vq}) \quad (17)$$

with  $\Gamma_0 = \frac{G_F M_{Z_L}^3}{24\sqrt{2}\pi}$ , here  $g_{Aq}$  and  $g_{Vq}$  are the axial-vector and effective vector couplings. The radiators  $R_{Aq}$  and  $R_{Vq}$  contain contributions from the final state gluons and photons. In the crudest approximation

$$R_{Vq} = R_{Aq} = 1 + \frac{\hat{\alpha}_s}{\pi} \quad (18)$$

where  $\alpha_s(q^2)$  is the QCD running coupling constant:

$$\hat{\alpha}_s \equiv \alpha_s(q^2 = M_{Z_L}^2) \quad (19)$$

The expression of the radiative correction to  $R_b$  can be expressed as [10]

$$\delta R_b \simeq \frac{2R_b^{SM}(1 - R_b^{SM})}{g_{Vb}^2(3 - \beta^2) + 2g_{Ab}^2\beta^2} [g_{Vb}(3 - \beta^2)\delta g_{Vb} + 2g_{Ab}\beta^2\delta g_{Ab}] \quad (20)$$

with  $\beta = \sqrt{1 - \frac{4\hat{m}_b^2}{M_{Z_L}^2}}$  being the velocity of b-quark in  $Z$  decay, here  $\hat{m}_b$  is the value of the running mass of the b-quark at scale  $M_{Z_L}$  calculated in  $\overline{MS}$  scheme [11].

The unpolarized forward-backward asymmetry in the decay to  $b\bar{b}$  equals:

$$A_{FB}^b = \frac{N_F - N_B}{N_F + N_B} \quad (21)$$

where  $N_F$  is the cross section for finding the scattered fermion in the hemisphere defined by the incident electron direction and  $N_B$  is the cross section for finding it in the positron hemisphere. It can be expressed as

$$A_{FB}^b = \frac{3}{4} \left(1 - \frac{k_A}{\pi}\right) A_e A_b \quad (22)$$

where the factor  $(1 - \frac{k_A}{\pi})$  represents a QCD radiative correction, as in Ref. [12], for which we use the numerical value 0.95,  $A_e$  refers to the creation of  $Z$  boson in  $e^+e^-$  -annihilation, while  $A_b$  is the left-right coupling constant asymmetry refers to its decay in  $b\bar{b}$  [9]

$$A_b = \frac{2g_{Ab}g_{Vb}}{\beta^2 g_{Ab}^2 + (3 - \beta^2)g_{Vb}^2/2} \quad (23)$$

The relevant Feynman diagrams for the LHT contributions are shown in Fig.1. We use the 't Hooft-Feynman gauge, so the contributions of Goldstone bosons should be involved. In our calculation,  $g_{Ab}$  and  $g_{Vb}$  should be replaced by  $\bar{g}_{Ab}$  and  $\bar{g}_{Vb}$ ,  $g_{V,A}^b + \delta g_{V,A}^{SM}$  can be found in Ref. [13]. The calculations of the loop diagrams are straightforward. Each loop diagram is composed of some scalar loop functions [14], which are calculated by using

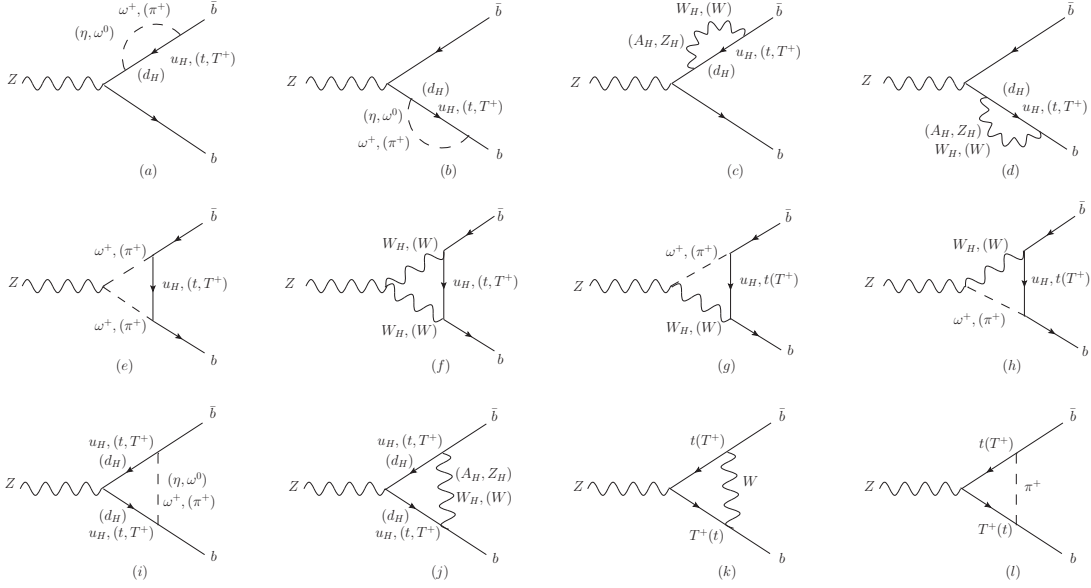


FIG. 1: Feynman diagrams of  $Z \rightarrow b\bar{b}$  at one-loop level in the LHT model.

LOOPTOOLS [15]. The relevant Feynman rules can be found in Ref. [16]. We applied the on-shell renormalization scheme and have checked that the divergences are canceled.

In the numerical calculations we take the input parameters [17] as Fermi constant  $G_F = 1.16637 \times 10^{-5} GeV^{-2}$ , the fine-structure constant  $\alpha = 1/128$ ,  $Z$ -boson mass  $M_{Z_L} = 91.2 GeV$ , fermion masses  $m_f$ , the electroweak mixing angle  $S_W^2 = 0.231$  and the final-state asymmetry parameter  $A_e = 0.1515$ . In our calculation, the relevant LHT parameters are the scale  $f$ , the mixing parameter  $x_L$ , the mirror quark masses and parameters in the matrices  $V_{Hu}$  and  $V_{Hd}$ .

For the mirror quark masses, from Eq.(5) we get  $m_{u_H^i} = m_{d_H^i}$  at  $\mathcal{O}(v/f)$  and further assume

$$m_{u_H^1} = m_{u_H^2} = m_{d_H^1} = m_{d_H^2} = M_{12}, m_{u_H^3} = m_{d_H^3} = M_3 \quad (24)$$

For the matrices  $V_{Hu}$  and  $V_{Hd}$ , considering the constraints in Ref.[18], we study the completely generic scenario, i.e.the six parameters of  $V_{Hd}$  are arbitrary. After that, we follow Ref.[19] to consider the following two scenarios for comparison:

Scenario I:  $V_{Hd} = 1, V_{Hu} = V_{CKM}^\dagger$

Scenario II:  $S_{13}^d = 0.5, \delta_{12}^d = \delta_{23}^d = 0, \delta_{13}^d = \delta_{13}^{SM}, S_{ij}^d = S_{ij}^{SM}$  otherwise

Firstly, we discuss the  $R_b$  changes with the LHT parameters, the numerical results are

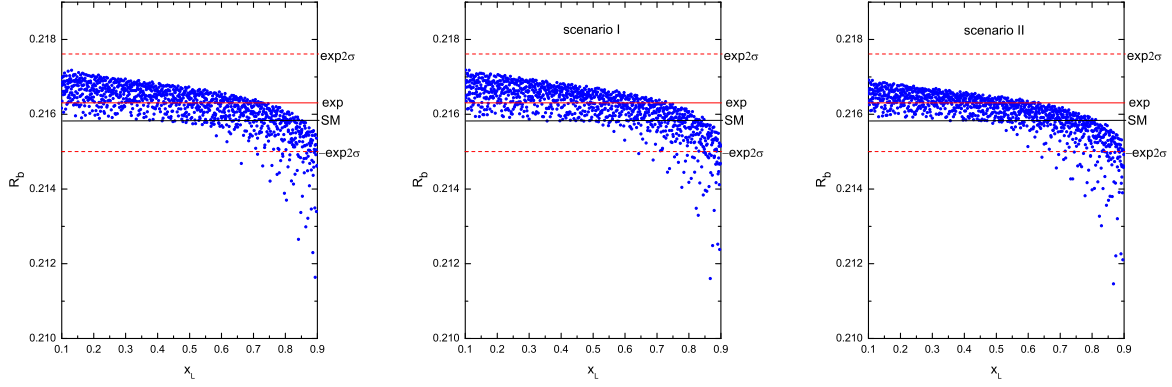


FIG. 2: Scatter plots of  $R_b$  versus  $x_L$  in arbitrary scenario, scenario I and scenario II, respectively. The experimental value  $R_b = 0.21629 \pm 0.00066$ .

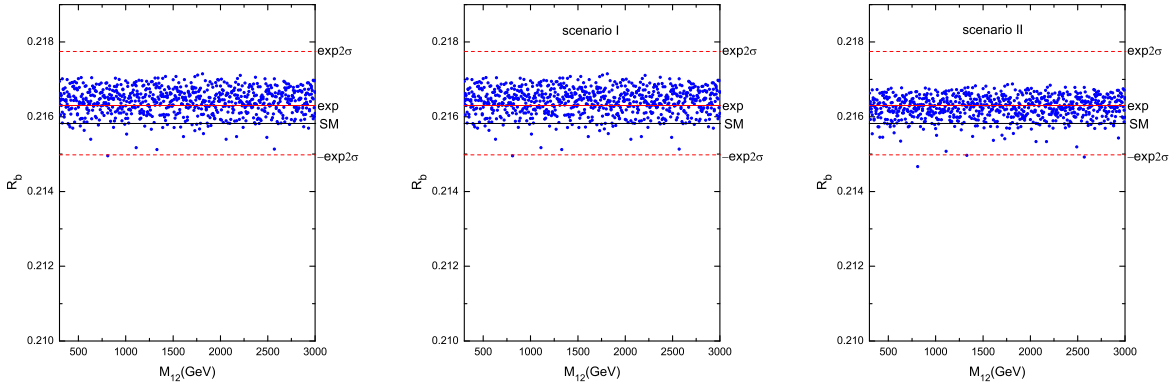


FIG. 3: Scatter plots of  $R_b$  versus  $M_{12}$  in three different scenarios, respectively. The experimental value  $R_b = 0.21629 \pm 0.00066$ .

summarized in Fig.(2-3). To see the influence of the mixing parameter  $x_L$  on the  $R_b$ , considering the existing constraints, we let the parameters vary randomly in the range:  $M_{12} = 300 \sim 3000 GeV$ ,  $M_3 = 300 \sim 3000 GeV$ ,  $f = 400 \sim 3000 GeV$ . In these three scenarios, we can see the plots of  $R_b$  decline with the  $x_L$  increasing, which shows that the contribution of the mixing diagrams between  $t$  and  $T^+$  is negative and becomes larger with the  $x_L$  increasing. When  $x_L > 0.7$ , part of the plots are beyond the  $2\sigma$  regions of its experimental value. This feature is similar in three different scenarios.

To see the influence of the first two generation mirror quarks mass  $M_{12}$  on the  $R_b$ ,



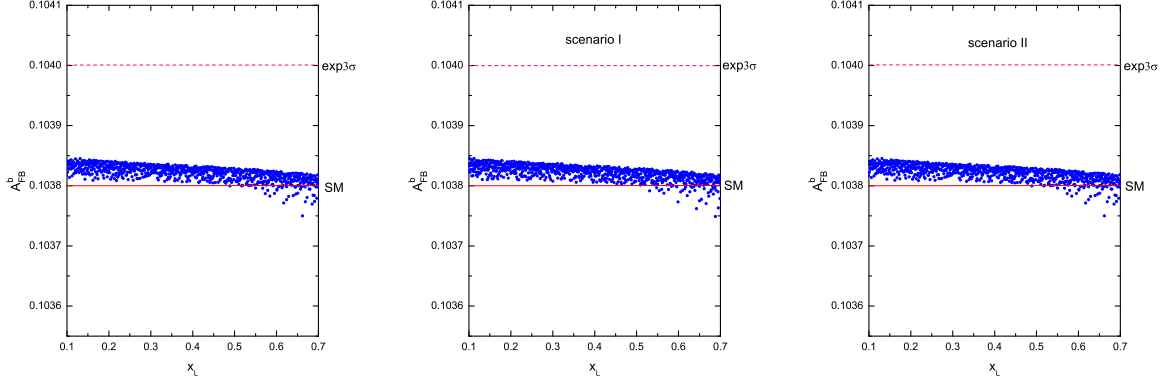


FIG. 4: Scatter plots of  $A_{FB}^b$  versus  $x_L$  in three different scenarios, respectively. The experimental value  $A_{FB}^b = 0.0992 \pm 0.0016$ .

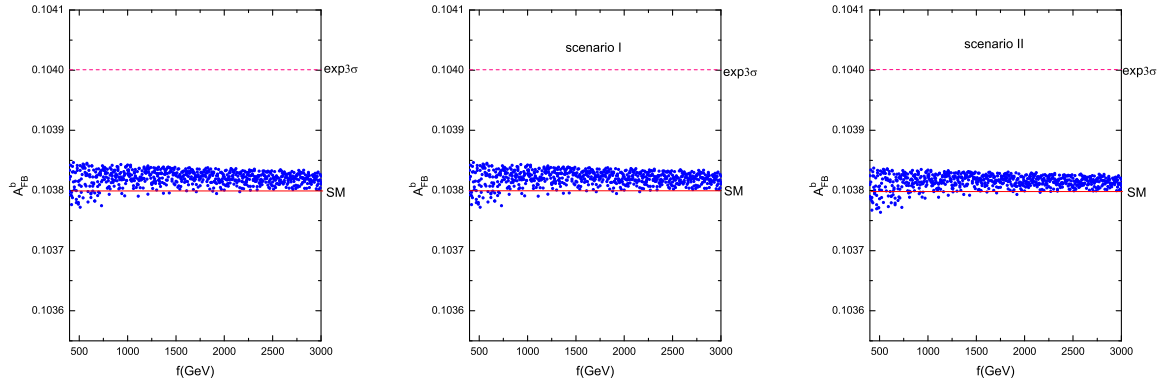


FIG. 5: Scatter plots of  $A_{FB}^b$  versus  $f$  in three different scenarios, respectively. The experimental value  $A_{FB}^b = 0.0992 \pm 0.0016$ .

considering the constraint from  $R_b$  on the  $x_L$ , we let the parameters vary randomly in the range:  $M_3 = 300 \sim 3000 GeV$ ,  $f = 400 \sim 3000 GeV$ ,  $x_L = 0.1 \sim 0.7$ . In these three scenarios, we can see the plots of  $R_b$  are almost in the  $2\sigma$  regions of its experimental value. The noticeable feature is that the  $R_b$  isn't sensitive to  $M_{12}$  so that the constraint from  $R_b$  on  $M_{12}$  is very loose.

Secondly, we discuss the  $A_{FB}^b$  changes with the LHT parameters, the numerical results are summarized in Fig.(4-6). Same as the  $R_b$ , the  $A_{FB}^b$  isn't sensitive to  $M_{12}$ , so we don't give the figures of the  $A_{FB}^b$  as the function of  $M_{12}$ . To see the influence of the

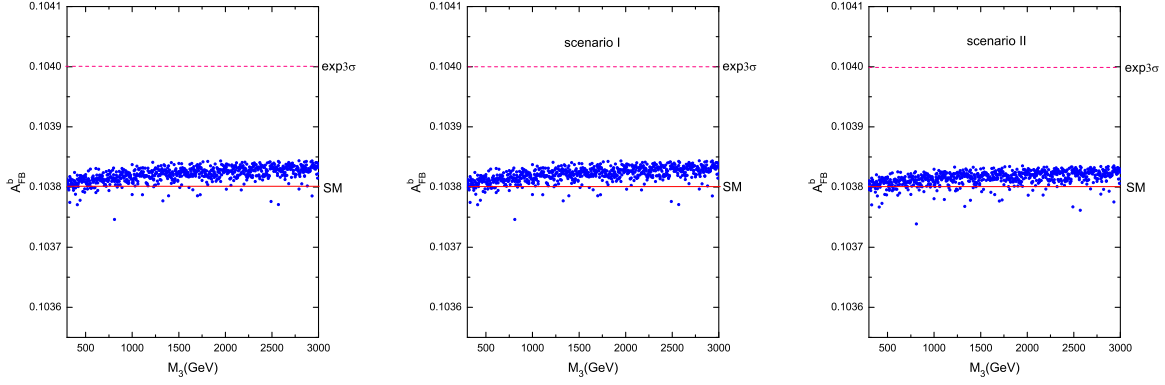


FIG. 6: Scatter plots of  $A_{FB}^b$  versus  $M_3$  in three different scenarios, respectively. The experimental value  $A_{FB}^b = 0.0992 \pm 0.0016$ .

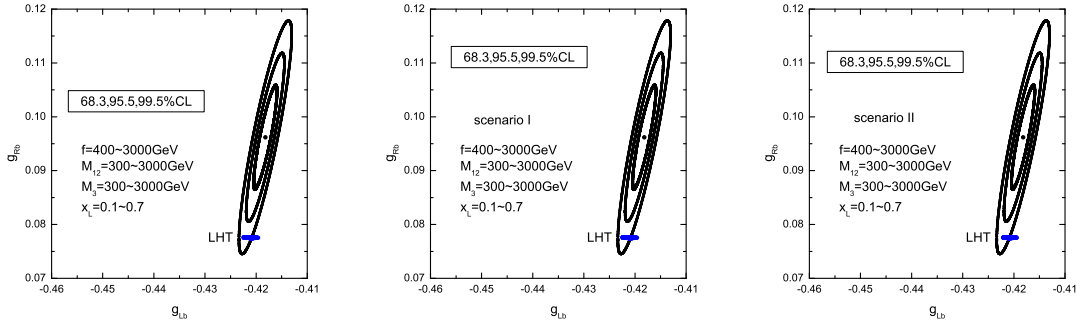


FIG. 7: The left-handed and right-handed coupling constants in the LHT model. The experimental value  $g_L^b = -0.4182 \pm 0.0015$ ,  $g_R^b = 0.0962 \pm 0.0063$ .

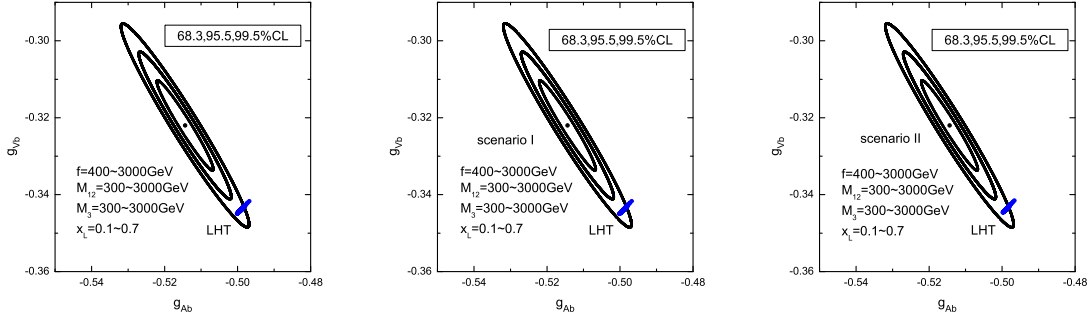


FIG. 8: The effective vector and axial-vector coupling constants in the LHT model. The experimental value  $g_V^b = -0.3220 \pm 0.0077$ ,  $g_A^b = -0.5144 \pm 0.0051$ .

mixing parameter  $x_L$  on the  $A_{FB}^b$ , we let the parameters vary randomly in the range:  $M_{12} = 300 \sim 3000 GeV$ ,  $M_3 = 300 \sim 3000 GeV$ ,  $f = 400 \sim 3000 GeV$ . For the same reason, we can see the plots of  $A_{FB}^b$  decline and become closer to the experimental central value with the  $x_L$  increasing. However, the contribution of the new particles is not large enough so that the plots of the  $A_{FB}^b$  are still entirely scattered between the  $2\sigma$  and  $3\sigma$  region of its experimental value.

To see the influence of the scale  $f$  on the  $A_{FB}^b$ , we let the parameters vary randomly in the range:  $M_{12} = 300 \sim 3000 GeV$ ,  $M_3 = 300 \sim 3000 GeV$ ,  $x_L = 0.1 \sim 0.7$ . We can see the plots of  $A_{FB}^b$  are entirely between the  $2\sigma$  and  $3\sigma$  region of its experimental value. The plots of  $A_{FB}^b$  become closer to the SM with the  $f$  increasing, which shows that the contribution of the heavy particles decouples with the  $f$  increasing.

To see the influence of the third generation mirror quarks mass  $M_3$  on the  $A_{FB}^b$ , we let the parameters vary randomly in the range:  $M_{12} = 300 \sim 3000 GeV$ ,  $f = 400 \sim 3000 GeV$ ,  $x_L = 0.1 \sim 0.7$ . We can see the plots of  $A_{FB}^b$  are entirely between the  $2\sigma$  and  $3\sigma$  region of its experimental value.

Finally, we discuss the  $Zbb$  couplings in the LHT model. In our calculation, we still consider the above three scenarios and let the parameters vary randomly in the range:  $M_{12} = 300 \sim 3000 GeV$ ,  $M_3 = 300 \sim 3000 GeV$ ,  $f = 400 \sim 3000 GeV$ ,  $x_L = 0.1 \sim 0.7$ , the numerical results are summarized in Figs.(7-8). We confirm the result of Ref.[18], in which the correction from the mixing diagrams between  $t$  and  $T^+$  to  $Zb\bar{b}$  couplings is mainly on the  $g_L^b$  and doesn't have the correct sign to alleviate the large deviation between theoretical predictions and experimental values. The plots scatter beyond the  $3\sigma$  region their experimental values are mainly caused by these couplings. Furthermore, the correction on the  $g_R^b$  is very small. However, there is a little difference when we consider the contributions involve other new particles. At this time, we can see part of the plots scatter in the  $3\sigma$  internal region of their experimental values, where the deviation of  $g_L^b$  can be alleviated. Unfortunately, the correction on the  $g_R^b$  is still very small and the plots still scatter near the  $3\sigma$  region of their experimental values so that the large deviation between theoretical predictions and experimental values can't be explained. The similar results are found on the  $g_A^b$  and  $g_V^b$ .

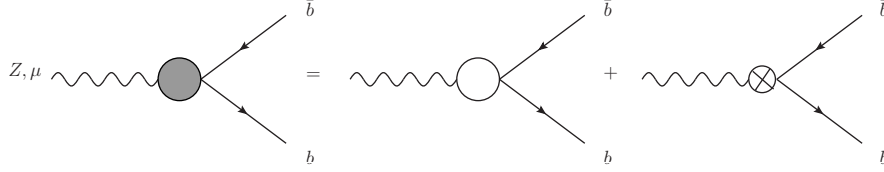
## IV. CONCLUSIONS

In this paper, we studied the one-loop contributions of the new particles to the  $R_b$  and  $A_{FB}^b$  for three different scenarios in the framework of the LHT model. From the scatter plots of  $R_b$  versus  $x_L$ , the precision measurement data of  $R_b$  can give strong constraint on the  $x_L$ . Considering this constraint, we can see  $R_b$  isn't sensitive to the mass of the first two generation mirror quarks. The relevant parameters are weakly constrained by the precision measurement data of  $A_{FB}^b$ . In the given parameters space, the large deviation of  $A_{FB}^b$  can't be explained reasonably. From our study, the LHT model can provide the correction to the  $g_L^b$  and have small part of the parameter space to alleviate the deviation between theoretical predictions and experimental values. But the LHT model can't provide the large correction to the  $g_R^b$  so that the large deviation between the SM prediction predictions and experimental values of the  $Zbb$  couplings can't be alleviated substantially.

### Acknowledgments

We would thank Junjie Cao and Lei Wu for useful discussions and providing the calculation programs. This work is supported by the National Natural Science Foundation of China under Grant Nos.10775039, 11075045, by Specialized Research Fund for the Doctoral Program of Higher Education under Grant No.20094104110001 and by HASTIT under Grant No.2009HASTIT004.

Appendix A: The expression of the renormalization vertex  $\hat{\Gamma}_{Zb\bar{b}}^\mu$  [20]



$$\begin{aligned}\hat{\Gamma}_{Zb\bar{b}}^\mu &= \Gamma_{Zb\bar{b}}^\mu - ie\gamma^\mu(v_b - a_b\gamma_5)\frac{C_W}{2S_W}\delta Z_{ZA} - ieQ_b\gamma^\mu\frac{1}{2}\delta Z_{ZA} \\ &\quad + ie\gamma^\mu(v_b - a_b\gamma_5)\delta Z_V^b - ie\gamma^\mu\gamma_5(v_b - a_b\gamma_5)\delta Z_A^b\end{aligned}$$

where

$$\begin{aligned}v_b &\equiv \frac{I_b^3 - 2Q_b S_W^2}{2C_W S_W}, \quad a_b \equiv \frac{I_b^3}{2C_W S_W}, \quad I_b^3 = -\frac{1}{2}, \quad Q_b = -\frac{1}{3} \\ \delta Z_{ZA} &= 2\frac{\Sigma_T^{AZ}(0)}{M_{Z_L}^2} \\ \delta Z_L^b &= Re\Sigma_L^b(m_b^2) + m_b^2\frac{\partial}{\partial P_b^2}Re[\Sigma_L^b(P_b^2) + \Sigma_R^b(P_b^2) + 2\Sigma_S^b(P_b^2)]|_{P_b^2=m_b^2} \\ \delta Z_R^b &= Re\Sigma_R^b(m_b^2) + m_b^2\frac{\partial}{\partial P_b^2}Re[\Sigma_L^b(P_b^2) + \Sigma_R^b(P_b^2) + 2\Sigma_S^b(P_b^2)]|_{P_b^2=m_b^2} \\ \delta Z_V^b &= \frac{1}{2}(\delta Z_L^b + \delta Z_R^b), \quad \delta Z_A^b = \frac{1}{2}(\delta Z_L^b - \delta Z_R^b)\end{aligned}$$

$$\begin{aligned}\hat{\Gamma}_{Zb\bar{b}}^{LHT,\mu} &= \Gamma_{Zb\bar{b}}^\mu(\pi^\pm) + \Gamma_{Zb\bar{b}}^\mu(\eta) + \Gamma_{Zb\bar{b}}^\mu(\omega^0) + \Gamma_{Zb\bar{b}}^\mu(\omega^\pm) + \Gamma_{Zb\bar{b}}^\mu(W_L^\pm) + \Gamma_{Zb\bar{b}}^\mu(A_H) + \Gamma_{Zb\bar{b}}^\mu(Z_H) \\ &\quad + \Gamma_{Zb\bar{b}}^\mu(W_H^\pm) + \Gamma_{Zb\bar{b}}^\mu(\pi^\pm, W_L^\pm) + \Gamma_{Zb\bar{b}}^\mu(\omega^\pm, W_H^\pm) + \delta\Gamma_{Zb\bar{b}}^\mu(\pi^\pm) + \delta\Gamma_{Zb\bar{b}}^\mu(\eta) + \delta\Gamma_{Zb\bar{b}}^\mu(\omega^0) \\ &\quad + \delta\Gamma_{Zb\bar{b}}^\mu(\omega^\pm) + \delta\Gamma_{Zb\bar{b}}^\mu(W_L^\pm) + \delta\Gamma_{Zb\bar{b}}^\mu(A_H) + \delta\Gamma_{Zb\bar{b}}^\mu(Z_H) + \delta\Gamma_{Zb\bar{b}}^\mu(W_H^\pm)\end{aligned}$$

## Appendix B: The explicit expressions of the $\delta g_{L,R}^{LHT}$

They can be represented in form of 1-point, 2-point and 3-point standard functions  $A, B_0, B_1, C_{ij}$ . Here  $P_b$  and  $\bar{P}_b$  are outgoing. In all expressions, the mass of b-quark is ignored.

$$\begin{aligned}
\delta g_L &= \frac{1}{16\pi^2} g^2 C_W^2 (V_{Hd})_{i3}^* (V_{Hd})_{i3} m_{u_H}^2 C_0^a \\
&\quad - \frac{1}{16\pi^2} \frac{g'^2}{100 M_{A_H}^2} (V_{Hd})_{i3}^* (V_{Hd})_{i3} \left\{ \left(-\frac{1}{2} + \frac{1}{3} S_W^2\right) [m_{d_H}^4 C_0^b - m_{d_H}^2 M_{Z_L}^2 C_{12}^b - m_{d_H}^2 M_{Z_L}^2 C_{23}^b \right. \\
&\quad - 2m_{d_H}^2 C_{24}^b + \frac{1}{2} m_{d_H}^2] - \frac{1}{2} \left[ \frac{1}{2} m_{d_H}^2 B_0(-P_b, m_{d_H}^i, M_{A_H}) \right. \\
&\quad \left. + \frac{1}{2} m_{d_H}^2 (m_{d_H}^2 - M_{A_H}^2) \frac{\partial}{\partial P_b^2} B_0(-P_b, m_{d_H}^i, M_{A_H}) \right] \\
&\quad \left. - \frac{1}{3} S_W^2 \left[ -\frac{1}{2} m_{d_H}^2 B_0(-P_b, m_{d_H}^i, M_{A_H}) - \frac{1}{2} m_{d_H}^2 (m_{d_H}^2 - M_{A_H}^2) \frac{\partial}{\partial P_b^2} B_0(-P_b, m_{d_H}^i, M_{A_H}) \right] \right\} \\
&\quad - \frac{1}{16\pi^2} \frac{g^2}{4 M_{Z_H}^2} (V_{Hd})_{i3}^* (V_{Hd})_{i3} \left\{ \left(-\frac{1}{2} + \frac{1}{3} S_W^2\right) [m_{d_H}^4 C_0^c - m_{d_H}^2 M_{Z_L}^2 C_{12}^c - m_{d_H}^2 M_{Z_L}^2 C_{23}^c \right. \\
&\quad - 2m_{d_H}^2 C_{24}^c + \frac{1}{2} m_{d_H}^2] - \frac{1}{2} \left[ \frac{1}{2} m_{d_H}^2 B_0(-P_b, m_{d_H}^i, M_{Z_H}) \right. \\
&\quad \left. + \frac{1}{2} m_{d_H}^2 (m_{d_H}^2 - M_{Z_H}^2) \frac{\partial}{\partial P_b^2} B_0(-P_b, m_{d_H}^i, M_{Z_H}) \right] - \frac{1}{3} S_W^2 \left[ -\frac{1}{2} m_{d_H}^2 B_0(-P_b, m_{d_H}^i, M_{Z_H}) \right. \\
&\quad \left. - \frac{1}{2} m_{d_H}^2 (m_{d_H}^2 - M_{Z_H}^2) \frac{\partial}{\partial P_b^2} B_0(-P_b, m_{d_H}^i, M_{Z_H}) \right] \right\} \\
&\quad - \frac{1}{16\pi^2} \frac{g^2}{2 M_{W_H}^2} (V_{Hd})_{i3}^* (V_{Hd})_{i3} \left\{ \left(\frac{1}{2} - \frac{2}{3} S_W^2\right) [m_{u_H}^4 C_0^d - m_{u_H}^2 M_{Z_L}^2 C_{12}^d - m_{u_H}^2 M_{Z_L}^2 C_{23}^d \right. \\
&\quad - 2m_{u_H}^2 C_{24}^d + \frac{1}{2} m_{u_H}^2] - \frac{1}{2} \left[ \frac{1}{2} m_{u_H}^2 B_0(-P_b, m_{u_H}^i, M_{W_H}) \right. \\
&\quad \left. + \frac{1}{2} m_{u_H}^2 (m_{u_H}^2 - M_{W_H}^2) \frac{\partial}{\partial P_b^2} B_0(-P_b, m_{u_H}^i, M_{W_H}) \right] - \frac{1}{3} S_W^2 \left[ -\frac{1}{2} m_{u_H}^2 B_0(-P_b, m_{u_H}^i, M_{W_H}) \right. \\
&\quad \left. - \frac{1}{2} m_{u_H}^2 (m_{u_H}^2 - M_{W_H}^2) \frac{\partial}{\partial P_b^2} B_0(-P_b, m_{u_H}^i, M_{W_H}) \right] + 2C_W^2 m_{u_H}^2 C_{24}^e \left. \right\} \\
&\quad - \frac{1}{16\pi^2} \frac{g'^2}{100} (V_{Hd})_{i3}^* (V_{Hd})_{i3} \left\{ \left(-\frac{1}{2} + \frac{1}{3} S_W^2\right) [-2m_{d_H}^2 C_0^f + 2M_{Z_L}^2 C_{11}^f + 2M_{Z_L}^2 C_{23}^f \right. \\
&\quad + 4C_{24}^f - 2] + \left[ \frac{1}{2} B_0(-P_b, m_{d_H}^i, M_{A_H}) + \frac{1}{2} (m_{d_H}^2 - M_{A_H}^2) \frac{\partial}{\partial P_b^2} B_0(-P_b, m_{d_H}^i, M_{A_H}) \right. \\
&\quad \left. - \frac{1}{3} S_W^2 B_0(-P_b, m_{d_H}^i, M_{A_H}) - \frac{1}{3} S_W^2 (m_{d_H}^2 - M_{A_H}^2) \frac{\partial}{\partial P_b^2} B_0(-P_b, m_{d_H}^i, M_{A_H}) \right] - \frac{1}{2} + \frac{1}{3} S_W^2 \left. \right\}
\end{aligned}$$

$$\begin{aligned}
& -\frac{1}{16\pi^2} \frac{g^2}{4} (V_{Hd})_{i3}^* (V_{Hd})_{i3} \left\{ \left(-\frac{1}{2} + \frac{1}{3} S_W^2\right) [-2m_{d_H}^2 C_0^g + 2M_{Z_L}^2 C_{11}^g + 2M_{Z_L}^2 C_{23}^g \right. \\
& + 4C_{24}^g - 2] + \left[\frac{1}{2} B_0(-P_b, m_{d_H}^i, M_{Z_H}) + \frac{1}{2} (m_{d_H}^2 - M_{Z_H}^2) \frac{\partial}{\partial P_b^2} B_0(-P_b, m_{d_H}^i, M_{Z_H}) \right. \\
& \left. - \frac{1}{3} S_W^2 B_0(-P_b, m_{d_H}^i, M_{Z_H}) - \frac{1}{3} S_W^2 (m_{d_H}^2 - M_{Z_H}^2) \frac{\partial}{\partial P_b^2} B_0(-P_b, m_{d_H}^i, M_{Z_H}) \right] - \frac{1}{2} + \frac{1}{3} S_W^2 \left. \right\} \\
& + \frac{1}{16\pi^2} \frac{g^2}{2} (V_{Hd})_{i3}^* (V_{Hd})_{i3} \left(\frac{1}{2} - \frac{2}{3} S_W^2\right) [2m_{u_H}^2 C_0^h + 2M_{Z_L}^2 C_{11}^h + 2M_{Z_L}^2 C_{23}^h + 4C_{24}^h - 2] \\
& + \frac{1}{16\pi^2} \frac{g^2}{2} (V_{Hd})_{i3}^* (V_{Hd})_{i3} C_W^2 [-2M_{Z_L}^2 C_0^i - 2M_{Z_L}^2 C_{11}^i - 2M_{Z_L}^2 C_{23}^i - 12C_{24}^i + 2] \\
& + \frac{1}{16\pi^2} \frac{g^2}{2} (V_{Hd})_{i3}^* (V_{Hd})_{i3} \left[\frac{1}{2} B_0(-P_b, m_{u_H}^i, M_{W_H}) + \frac{1}{2} (m_{u_H}^2 - m_{W_H}^2) \frac{\partial}{\partial P_b^2} B_0(-P_b, m_{u_H}^i, M_{W_H}) \right. \\
& \left. - \frac{1}{3} S_W^2 B_0(-P_b, m_{u_H}^i, M_{W_H}) - \frac{1}{3} S_W^2 (m_{u_H}^2 - M_{W_H}^2) \frac{\partial}{\partial P_b^2} B_0(-P_b, m_{u_H}^i, M_{W_H}) - \frac{1}{2} + \frac{1}{3} S_W^2 \right] \\
& + \frac{1}{16\pi^2} \frac{g^2}{M_{Z_L}^2} C_W^2 [-2A(M_{W_H}) + 2M_{W_H}^2 B_0(0, M_{W_H}, M_{W_H}) + 2M_{W_H}^2 + M_{Z_L}^2 B_0(0, M_{W_H}, M_{W_H})] \\
& - \frac{1}{16\pi^2} \frac{2g^2}{M_{Z_L}^2} \left\{ \frac{2}{3} \left(\frac{1}{2} - \frac{2}{3} S_W^2\right) \left[-\frac{2}{3} A(m_{u_H}^i) + \frac{2}{3} m_{u_H}^2 B_0(0, m_{u_H}^i, m_{u_H}^i) + \frac{2}{3} m_{u_H}^2 \right] \right. \\
& - \frac{1}{3} \left(-\frac{1}{2} + \frac{1}{3} S_W^2\right) \left[-\frac{2}{3} A(m_{d_H}^i) + \frac{2}{3} m_{d_H}^2 B_0(0, m_{d_H}^i, m_{d_H}^i) + \frac{2}{3} m_{d_H}^2 \right] \\
& \left. - \left(-\frac{1}{2} + S_W^2\right) \left[-\frac{2}{3} A(m_{l_H}^i) + \frac{2}{3} m_{l_H}^2 B_0(0, m_{l_H}^i, m_{l_H}^i) + \frac{2}{3} m_{l_H}^2 \right] \right\} \\
& + \frac{g^2 x_L^2}{4M_{W_L}^2} (1 - 2S_W^2) \frac{v^2}{f^2} (V_{CKM})_{tb}^* (V_{CKM})_{tb} \frac{1}{16\pi^2} [-2m_{T^+}^2 + C_{24}^j] \\
& + \frac{g^2 x_L^2}{2M_{W_L}^2} \frac{v^2}{f^2} (V_{CKM})_{tb}^* (V_{CKM})_{tb} \frac{1}{16\pi^2} \left[\frac{2}{3} S_W^2 m_{T^+}^4 C_0^k - m_{T^+}^2 M_{Z_L}^2 C_{12}^k - \frac{2}{3} S_W^2 m_{T^+}^2 C_{23}^k \right. \\
& \left. - \frac{4}{3} S_W^2 C_{24}^k + \frac{1}{3} S_W^2 m_{T^+}^2 \right] \\
& + \frac{g^2 x_L^2}{4M_{W_L}^2} \frac{v^2}{f^2} (V_{CKM})_{tb}^* (V_{CKM})_{tb} \frac{1}{16\pi^2} \left\{ \frac{1}{2} m_{T^+}^2 B_0(-P_b, m_{T^+}, M_{W_L}) \right. \\
& \left. + \frac{1}{2} m_{T^+}^2 (m_{T^+}^2 - M_{W_L}^2) \frac{\partial}{\partial P_b^2} B_0(-P_b, m_{T^+}, M_{W_L}) \right. \\
& \left. - \frac{1}{3} S_W^2 [m_{T^+}^2 B_0(-P_b, m_{T^+}, M_{W_L}) + m_{T^+}^2 (m_{T^+}^2 - M_{W_L}^2) \frac{\partial}{\partial P_b^2} B_0(-P_b, m_{T^+}, M_{W_L})] \right\} \\
& + \frac{g^2 x_L^2}{4M_{W_L}^2} \frac{v^2}{f^2} (V_{CKM})_{tb}^* (V_{CKM})_{tb} \frac{1}{16\pi^2} [-m_{T^+}^2 + m_t^2 C_0^l] \\
& + \frac{g^2 x_L^2}{4M_{W_L}^2} \frac{v^2}{f^2} (V_{CKM})_{tb}^* (V_{CKM})_{tb} \frac{1}{16\pi^2} [-m_{T^+}^2 + m_t^2 C_0^m] \\
& + \frac{g^2 x_L^2}{2} C_W^2 \frac{v^2}{f^2} (V_{CKM})_{tb}^* (V_{CKM})_{tb} \frac{1}{16\pi^2} [-2M_{Z_L}^2 C_0^j - 2M_{Z_L}^2 C_{11}^j - 2M_{Z_L}^2 C_{23}^j - 12C_{24}^j + 2] \\
& + \frac{g^2 x_L^2}{2} \frac{v^2}{f^2} (V_{CKM})_{tb}^* (V_{CKM})_{tb} \frac{1}{16\pi^2} \frac{2}{3} S_W^2 [m_{T^+}^2 C_0^k - 2M_{Z_L}^2 C_{11}^k - 2M_{Z_L}^2 C_{23}^k - \frac{4}{3} C_{24}^k + 2]
\end{aligned}$$

$$\begin{aligned}
& + \frac{g^2 x_L^2 v^2}{4 f^2} (V_{CKM})_{tb}^* (V_{CKM})_{tb} \frac{1}{16\pi^2} [2M_{Z_L}^2 C_{11}^l + 2M_{Z_L}^2 C_{23}^l + 4C_{24}^l - 2] \\
& + \frac{g^2 x_L^2 v^2}{4 f^2} (V_{CKM})_{tb}^* (V_{CKM})_{tb} \frac{1}{16\pi^2} [2M_{Z_L}^2 C_{11}^m + 2M_{Z_L}^2 C_{23}^m + 4C_{24}^m - 2] \\
& + \frac{g^2 x_L^2 v^2}{2 f^2} (V_{CKM})_{tb}^* (V_{CKM})_{tb} \frac{1}{16\pi^2} \left[ \frac{1}{2} B_0(-P_b, m_{T^+}, M_{W_L}) \right. \\
& + (m_{T^+}^2 - M_{W_L}^2) \frac{\partial}{\partial P_b^2} B_0(-P_b, m_{T^+}, M_{W_L}) - \frac{1}{3} S_W^2 B_0(-P_b, m_{T^+}, M_{W_L}) \\
& \left. - \frac{1}{3} S_W^2 (m_{T^+}^2 - M_{W_L}^2) \frac{\partial}{\partial P_b^2} B_0(-P_b, m_{T^+}, M_{W_L}) - \frac{1}{2} + \frac{1}{3} S_W^2 \right] \\
& - \frac{g^2 x_L^2 v^2}{2 f^2} (V_{CKM})_{tb}^* (V_{CKM})_{tb} \frac{1}{16\pi^2} \left[ \frac{2}{3} S_W^2 m_{T^+}^2 C_0^n + 2 \left( 1 - \frac{2}{3} S_W^2 \right) M_{Z_L}^2 C_{11}^n \right. \\
& \left. + 2 \left( 1 - \frac{2}{3} S_W^2 \right) M_{Z_L}^2 C_{23}^n + 4 \left( 1 - \frac{2}{3} S_W^2 \right) C_{24}^n - 2 \left( 1 - \frac{2}{3} S_W^2 \right) \right] \\
& - \frac{g^2 x_L^2 v^2}{2 f^2} C_W^2 (V_{CKM})_{tb}^* (V_{CKM})_{tb} \frac{1}{16\pi^2} [-2M_{Z_L}^2 C_0^o - 2M_{Z_L}^2 C_{11}^o - 2M_{Z_L}^2 C_{23}^o - 12C_{24}^o + 2] \\
& - \frac{g^2 x_L^2 v^2}{2 f^2} (V_{CKM})_{tb}^* (V_{CKM})_{tb} \frac{1}{16\pi^2} \left[ \frac{1}{2} B_0(-P_b, m_t, M_{W_L}) + \frac{1}{2} (m_t^2 - M_{W_L}^2) \frac{\partial}{\partial P_b^2} B_0(-P_b, m_t, M_{W_L}) \right. \\
& \left. - \frac{1}{3} S_W^2 B_0(-P_b, m_t, M_{W_L}) - \frac{1}{3} S_W^2 (m_t^2 - M_{W_L}^2) \frac{\partial}{\partial P_b^2} B_0(-P_b, m_t, M_{W_L}) - \frac{1}{2} + \frac{1}{3} S_W^2 \right] \\
& - \frac{g^2 x_L^2 v^2}{2 M_{W_L}^2 f^2} (V_{CKM})_{tb}^* (V_{CKM})_{tb} \frac{1}{16\pi^2} \left[ -m_t^4 \left( 1 - \frac{2}{3} S_W^2 \right) C_0^o - m_t^2 M_{Z_L}^2 C_{12}^o \right. \\
& \left. - \frac{2}{3} S_W^2 m_t^2 M_{Z_L}^2 C_{23}^o - \frac{4}{3} m_t^2 S_W^2 C_{24}^o(\bar{P}_b, P_b, m_t, M_{W_L}, m_t) + \frac{1}{3} S_W^2 m_t^2 \right] \\
& - \frac{g^2 x_L^2 v^2}{4 M_{W_L}^2} (1 - 2S_W^2) \frac{v^2}{f^2} (V_{CKM})_{tb}^* (V_{CKM})_{tb} \frac{1}{16\pi^2} [-2m_t^2 C_{24}^o] \\
& - \frac{g^2 x_L^2 v^2}{4 M_{W_L}^2 f^2} (V_{CKM})_{tb}^* (V_{CKM})_{tb} \frac{1}{16\pi^2} m_t^2 \left\{ \frac{1}{2} B_0(-P_b, m_t, M_{W_L}) \right. \\
& \left. + \frac{1}{2} (m_t^2 - M_{W_L}^2) \frac{\partial}{\partial P_b^2} B_0(-P_b, m_t, M_{W_L}) \right. \\
& \left. - \frac{1}{3} S_W^2 [B_0(-P_b, m_t, M_{W_L}) + (m_t^2 - M_{W_L}^2) \frac{\partial}{\partial P_b^2} B_0(-P_b, m_t, M_{W_L})] \right\} \\
& - \frac{g^2 x_L^2 v^2}{2 f^2} S_W^2 (V_{CKM})_{tb}^* (V_{CKM})_{tb} \frac{1}{16\pi^2} [m_{T^+}^2 C_0^j(\bar{P}_b, P_b, M_{W_L}, m_{T^+}, M_{W_L})] \\
& - \frac{g^2 x_L^2 v^2}{2 f^2} S_W^2 (V_{CKM})_{tb}^* (V_{CKM})_{tb} \frac{1}{16\pi^2} [m_{T^+}^2 C_0^j(\bar{P}_b, P_b, M_{W_L}, m_{T^+}, M_{W_L})] \\
& + \frac{g^2 x_L^2 v^2}{2 f^2} S_W^2 (V_{CKM})_{tb}^* (V_{CKM})_{tb} \frac{1}{16\pi^2} [m_t^2 C_0^o(\bar{P}_b, P_b, M_{W_L}, m_t, M_{W_L})] \\
& + \frac{g^2 x_L^2 v^2}{2 f^2} S_W^2 (V_{CKM})_{tb}^* (V_{CKM})_{tb} \frac{1}{16\pi^2} [m_t^2 C_0^o(\bar{P}_b, P_b, M_{W_L}, m_t, M_{W_L})]
\end{aligned}$$



$$\begin{aligned}
C_{ij}^a &= C_{ij}^a(\bar{P}_b, P_b, M_{W_H}, m_{u_H^i}, M_{W_H}) \\
C_{ij}^b &= C_{ij}^b(\bar{P}_b, P_b, m_{d_H^i}, M_{A_H}, m_{d_H^i}) \\
C_{ij}^c &= C_{ij}^c(\bar{P}_b, P_b, m_{d_H^i}, M_{Z_H}, m_{d_H^i}) \\
C_{ij}^d &= C_{ij}^d(\bar{P}_b, P_b, m_{u_H^i}, M_{W_H}, m_{u_H^i}) \\
C_{ij}^e &= C_{ij}^e(\bar{P}_b, P_b, M_{W_H}, m_{u_H^i}, M_{W_H}) \\
C_{ij}^f &= C_{ij}^f(\bar{P}_b, P_b, m_{d_H^i}, M_{A_H}, m_{d_H^i}) \\
C_{ij}^g &= C_{ij}^g(\bar{P}_b, P_b, m_{d_H^i}, M_{Z_H}, m_{d_H^i}) \\
C_{ij}^h &= C_{ij}^h(\bar{P}_b, P_b, m_{u_H^i}, M_{W_H}, m_{u_H^i}) \\
C_{ij}^i &= C_{ij}^i(\bar{P}_b, P_b, M_{W_H}, m_{u_H^i}, M_{W_H}) \\
C_{ij}^j &= C_{ij}^j(\bar{P}_b, P_b, M_{W_L}, m_{T^+}, M_{W_L}) \\
C_{ij}^k &= C_{ij}^k(\bar{P}_b, P_b, m_{T^+}, M_{W_L}, m_{T^+}) \\
C_{ij}^l &= C_{ij}^l(\bar{P}_b, P_b, m_t, M_{W_L}, m_{T^+}) \\
C_{ij}^m &= C_{ij}^m(\bar{P}_b, P_b, m_{T^+}, M_{W_L}, m_t) \\
C_{ij}^n &= C_{ij}^n(\bar{P}_b, P_b, m_t, M_{W_L}, m_t) \\
C_{ij}^o &= C_{ij}^o(\bar{P}_b, P_b, M_{W_L}, m_t, M_{W_L})
\end{aligned}$$

$$\begin{aligned}
\delta g_R = & -\frac{1}{16\pi^2} \frac{g^2}{100M_{A_H}^2} (V_{Hd})_{i3}^* (V_{Hd})_{i3} \left\{ \frac{1}{3} S_W^2 m_{d_H}^2 B_1(-P_b, m_{d_H}, M_{A_H}) \right. \\
& - \frac{1}{3} S_W^2 \left[ -\frac{1}{2} m_{d_H}^2 B_0(-P_b, m_{d_H}, M_{A_H}) - \frac{1}{2} m_{d_H}^2 (m_{d_H}^2 - M_{A_H}^2) \frac{\partial}{\partial P_b^2} B_0(-P_b, m_{d_H}, M_{A_H}) \right] \left. \right\} \\
& - \frac{1}{16\pi^2} \frac{g^2}{4M_{Z_H}^2} (V_{Hd})_{i3}^* (V_{Hd})_{i3} \left\{ \frac{1}{3} S_W^2 m_{d_H}^2 B_1(-P_b, m_{d_H}, M_{Z_H}) \right. \\
& - \frac{1}{3} S_W^2 \left[ -\frac{1}{2} m_{d_H}^2 B_0(-P_b, m_{d_H}, M_{Z_H}) - \frac{1}{2} m_{d_H}^2 (m_{d_H}^2 - M_{Z_H}^2) \frac{\partial}{\partial P_b^2} B_0(-P_b, m_{d_H}, M_{Z_H}) \right] \left. \right\} \\
& + \frac{1}{16\pi^2} \frac{g^2}{2M_{W_H}^2} (V_{Hd})_{i3}^* (V_{Hd})_{i3} \left\{ \frac{1}{3} S_W^2 m_{u_H}^2 B_1(-P_b, m_{u_H}, M_{W_H}) \right. \\
& - \frac{1}{3} S_W^2 \left[ -\frac{1}{2} m_{u_H}^2 B_0(-P_b, m_{u_H}, M_{W_H}) - \frac{1}{2} m_{u_H}^2 (m_{u_H}^2 - M_{W_H}^2) \frac{\partial}{\partial P_b^2} B_0(-P_b, m_{u_H}, M_{W_H}) \right] \left. \right\} \\
& - \frac{1}{16\pi^2} \frac{g^2}{100} (V_{Hd})_{i3}^* (V_{Hd})_{i3} \left\{ \frac{2}{3} S_W^2 B_1(-P_b, m_{d_H}, M_{A_H}) + \frac{1}{3} S_W^2 B_0(-P_b, m_{d_H}, M_{A_H}) \right. \\
& + \frac{1}{3} S_W^2 (m_{d_H}^2 - M_{A_H}^2) \frac{\partial}{\partial P_b^2} B_0(-P_b, m_{d_H}, M_{A_H}) \left. \right\} \\
& - \frac{1}{16\pi^2} \frac{g^2}{4} (V_{Hd})_{i3}^* (V_{Hd})_{i3} \left\{ \frac{2}{3} S_W^2 B_1(-P_b, m_{d_H}, M_{Z_H}) + \frac{1}{3} S_W^2 B_0(-P_b, m_{d_H}, M_{Z_H}) \right. \\
& + \frac{1}{3} S_W^2 (m_{d_H}^2 - M_{Z_H}^2) \frac{\partial}{\partial P_b^2} B_0(-P_b, m_{d_H}, M_{Z_H}) \left. \right\} \\
& - \frac{1}{16\pi^2} \frac{g^2}{2} (V_{Hd})_{i3}^* (V_{Hd})_{i3} \left\{ \frac{2}{3} S_W^2 B_1(-P_b, m_{u_H}, M_{W_H}) + \frac{1}{3} S_W^2 B_0(-P_b, m_{u_H}, M_{W_H}) \right. \\
& + \frac{1}{3} S_W^2 (m_{u_H}^2 - M_{W_H}^2) \frac{\partial}{\partial P_b^2} B_0(-P_b, m_{u_H}, M_{W_H}) \left. \right\} \\
& + \frac{g^2 x_L^2}{4M_{W_L}^2} \frac{v^2}{f^2} (V_{CKM})_{tb}^* (V_{CKM})_{tb} \frac{1}{16\pi^2} \left\{ -\frac{2}{3} S_W^2 m_{T^+}^2 B_1(-P_b, m_{T^+}, M_{W_L}) \right. \\
& - \frac{2}{3} S_W^2 \left[ \frac{1}{2} m_{T^+}^2 B_0(-P_b, m_{T^+}, M_{W_L}) + \frac{1}{2} m_{T^+}^2 (m_{T^+}^2 - M_{W_L}^2) \frac{\partial}{\partial P_b^2} B_0(-P_b, m_{T^+}, M_{W_L}) \right] \left. \right\} \\
& + \frac{g^2 x_L^2}{2} \frac{v^2}{f^2} (V_{CKM})_{tb}^* (V_{CKM})_{tb} \frac{1}{16\pi^2} \left\{ -\frac{2}{3} S_W^2 B_1(-P_b, m_{T^+}, M_{W_L}) \right. \\
& - \frac{1}{3} S_W^2 \left[ B_0(-P_b, m_{T^+}, M_{W_L}) + (m_{T^+}^2 - M_{W_L}^2) \frac{\partial}{\partial P_b^2} B_0(-P_b, m_{T^+}, M_{W_L}) \right] \left. \right\} \\
& - \frac{g^2 x_L^2}{4M_{W_L}^2} \frac{v^2}{f^2} (V_{CKM})_{tb}^* (V_{CKM})_{tb} \frac{1}{16\pi^2} \left\{ -\frac{2}{3} S_W^2 m_t^2 B_1(-P_b, m_t, M_{W_L}) \right. \\
& - \frac{1}{3} S_W^2 \left[ m_t^2 B_0(-P_b, m_t, M_{W_L}) + m_t^2 (m_t^2 - M_{W_L}^2) \frac{\partial}{\partial P_b^2} B_0(-P_b, m_t, M_{W_L}) \right] \left. \right\} \\
& - \frac{g^2 x_L^2}{2} \frac{v^2}{f^2} (V_{CKM})_{tb}^* (V_{CKM})_{tb} \frac{1}{16\pi^2} \left\{ -\frac{2}{3} S_W^2 B_1(-P_b, m_t, M_{W_L}) \right. \\
& - \frac{1}{3} S_W^2 \left[ B_0(-P_b, m_t, M_{W_L}) + (m_t^2 - M_{W_L}^2) \frac{\partial}{\partial P_b^2} B_0(-P_b, m_t, M_{W_L}) \right] \left. \right\}
\end{aligned}$$

- 
- [1] N. Arkani-Hamed, A. G. Cohen, and H. Georgi, Phys. Lett. B 513, 232 (2001); N. Arkani-Hamed, et al., JHEP 0208, 020 (2002); JHEP 0208, 021 (2002); I. Low, W. Skiba, and D. Smith, Phys. Rev. D 66, 072001 (2002); D. E. Kaplan and M. Schmaltz, JHEP 0310, 039(2003).
- [2] N. Arkani-Hamed, A. G. Cohen, E. Katz, and A. E. Nelson, JHEP 0207, 034 (2002); S. Chang, JHEP 0312, 057 (2003); T. Han, H. E. Logan, B. McElrath, and L. T. Wang, Phys. Rev. D 67, 095004 (2003); M. Schmaltz and D. Tucker-smith, Ann. Rev. Nucl. Part. Sci. 55,229 (2005).
- [3] C. Csaki, J. Hubisz, G. D. Kribs, P. Meade, J. Terning, Phys. Rev. D 67, 115002 (2003); Phys. Rev. D 68, 035009 (2003); J. L. Hewett, F. J. Petriello, and T. G. Rizzo, JHEP 0310, 062 (2003); M. C. Chen and S. Dawson, Phys. Rev. D 70, 015003 (2004); M. C. Chen, et al., Mod. Phys. Lett. A 21, 621 (2006); W. Kilian and J. Reuter, Phys. Rev. D 70, 015004 (2004).
- [4] G. Marandella, C. Schappacher and A. Strumia, Phys. Rev. D 72, 035014 (2005).
- [5] H. C. Cheng and I. Low, JHEP 0309, 051 (2003); JHEP 0408, 061 (2004); I. Low, JHEP 0410, 067 (2004); J. Hubisz and P. Meade, Phys. Rev. D 71, 035016 (2005).
- [6] D. Comelli and J. P. Silva, Phys. Rev. D 54(1996)1176; V. D. Barger, K. M. Cheung, P. Langaclar, Phys. Lett. B 381(1996)226; P. Bamert, C. P. Burgess, J. M. Cline, D. London, and E. Nardi, Phys. Rev. D 54(1996)4275; D. Atwood, L. Reina, and A. Soni, Phys. Rev. D 54(1996)3296.
- [7] The ALEPH, CDF, D0, DELPHI, L3, OPAL, SLD Collaborations, the LEP Electroweak Working Group, the Tevatron Electroweak Working Group, and the SLD electroweak and heavy flavour groups, arXiv:0811.4682v1 [hep-ex] 28 Nov 2008.
- [8] M. Blanke, et al., Phys. Lett. B 646, 253 (2007).
- [9] V. A. Novikov, L. B. Okun, A. N. Rozanov, M. I. Vysotsky, Rept. Prog. Phys. 62.1275-1332(1999); Morris L. Swartz, Int. J. Mod. Phys. A 15S1 307-332(2000).
- [10] M. Boulware and D. Finnell, Phys. Rev. D 44, 2054 (1991); Junjie Cao, Zhaohua Xiong and Jin Min Yang, Phys. Rev. Lett. 88, 111802 (2002).

- [11] N.Gray,David J. Broadhurst, W. Grafe, K. Schilcher., Z.Phys. C48:673-680 (1990) 673;L.R. Surguladze,Phys.Lett. B341:60-72(1994).
- [12] M.E. Peskin and T. Takeuchi, Phys. Rev. D46,381(1992).
- [13] The ALEPH,DELPHI, L3, OPAL, SLD Collaborations,the LEP Electroweak Working Group,the SLD Electroweak and Heavy Flavour Groups,Phys.Rept.427:257(2006).
- [14] G. t Hooft and M. J. G. Veltman,Nucl. Phys. B 153, 365 (1979).
- [15] T. Hahn and M. Perez-Victoria, Computl. Phys. Commun. 118, 153 (1999); T. Hahn, Nucl. Phys. Proc. Suppl. 135, 333 (2004).
- [16] M.Blanke, et al., JHEP 0701:066 (2007).
- [17] C. AMSLER, et al., Phys. Lett. B 667,1 (2008).
- [18] J.Hubisz, P.Meade, A.Noble, M.Perelstein,JHEP 0601:135(2006).
- [19] J.Hubisz, S. J. Lee, and G. Paz, JHEP 0606:041 (2006).
- [20] W.F.L.Hollik,Preprint,DESY 88-188(1988); A.Denner, Fortschr.Phys.41: 307-420 (1993).